

Filipa M. A. Valente · A. Sofia F. Oliveira
Nicole Gnadl · Isabel Pacheco · Ana V. Coelho
António V. Xavier · Miguel Teixeira
Cláudio M. Soares · Inês A. C. Pereira

Hydrogenases in *Desulfovibrio vulgaris* Hildenborough: structural and physiologic characterisation of the membrane-bound [NiFeSe] hydrogenase

Received: 15 May 2005 / Accepted: 11 August 2005 / Published online: 27 September 2005
© SBIC 2005

Abstract The genome of *Desulfovibrio vulgaris* Hildenborough (*DvH*) encodes for six hydrogenases (Hases), making it an interesting organism to study the role of these proteins in sulphate respiration. In this work we address the role of the [NiFeSe] Hase, found to be the major Hase associated with the cytoplasmic membrane. The purified enzyme displays interesting catalytic properties, such as a very high H₂ production activity, which is dependent on the presence of phospholipids or detergent, and resistance to oxygen inactivation since it is isolated aerobically in a Ni(II) oxidation state. Evidence was obtained that the [NiFeSe] Hase is post-translationally modified to include a hydrophobic group bound to the N-terminal, which is responsible for its membrane association. Cleavage of this group originates a soluble, less active form of the enzyme. Sequence analysis shows that [NiFeSe] Hases from *Desulfovibrionaceae* form a separate family from the [NiFe] enzymes of these organisms, and are more closely related to [NiFe] Hases from more distant bacterial species that have a medial [4Fe4S]^{2+/1+} cluster, but not a selenocysteine. The interaction of the [NiFeSe] Hase with periplasmic cytochromes was investigated and is similar to the [NiFe]_I Hase, with the Type I cytochrome *c*₃ as the preferred electron acceptor. A model of the *DvH*

[NiFeSe] Hase was generated based on the structure of the *Desulfomicrobium baculatum* enzyme. The structures of the two [NiFeSe] Hases are compared with the structures of [NiFe] Hases, to evaluate the consensual structural differences between the two families. Several conserved residues close to the redox centres were identified, which may be relevant to the higher activity displayed by [NiFeSe] Hases.

Keywords Hydrogenases · Cytochromes · Sulphate-reducing bacteria · Electron transfer

Abbreviations *DvH*: *D. vulgaris* Hildenborough · *Dm*: *Desulfomicrobium* · Hase: Hydrogenase · [NiFeSe]_m: Membrane-bound form of the [NiFeSe] Hase · [NiFeSe]_s: Soluble form of the [NiFeSe] Hase · TpI *c*₃: Type I cytochrome *c*₃ · TpII *c*₃: Type II cytochrome *c*₃ · HmcA: 16-haem high molecular weight cytochrome *c*

Electronic Supplementary Material Supplementary material is available for this article at <http://dx.doi.org/10.1007/s00775-005-0022-4>

F. M. A. Valente · A. S. F. Oliveira · N. Gnadl · I. Pacheco
A. V. Coelho · A. V. Xavier · M. Teixeira · C. M. Soares
I. A. C. Pereira (✉)
Instituto de Tecnologia Química e Biológica,
Universidade Nova de Lisboa, Oeiras, Portugal
E-mail: ipereira@itqb.unl.pt
Tel.: +351-214-469327
Fax: +351-214-411277

A. V. Coelho
Departamento de Química,
Universidade de Évora,
Évora, Portugal

Introduction

Hydrogen is regarded as the fuel of the future. Recently, there has been a renewed interest in the biological production of hydrogen, due to its potential as a sustainable source which can be harvested from organic wastes [1–4]. Biological hydrogen conversion is carried out by hydrogenases (Hases), enzymes that catalyse the production and/or consumption of H₂ at a complex binuclear metal centre deeply buried within the protein [5]. Research on Hases aims to understand the catalytic mechanism and structural determinants for its activity, and holds the promise for the development of oxygen-stable engineered proteins (or derived synthetic catalysts) that may be used as alternatives to platinum in fuel cells [6], as well as in several other biotechnological applications [7]. Hases play a central role in the energy metabolism of microbial organisms, in several possible metabolic contexts [8]. For many microorganisms, both

aerobic and anaerobic, H₂ can serve as an energy source for respiratory metabolism and/or carbon fixation, whereas in fermentative organisms H₂ formation is a way of disposing of excess-reducing power. Some organisms, like nitrogen fixers and sulphate-reducing bacteria (SRB), carry out both processes by recycling the H₂ produced, in order to avoid energy loss and/or as an indirect process for achieving energy conservation [9].

There are two, phylogenetically distinct, main classes of Hases: the [NiFe] and the [FeFe] Hases [10, 11], the first having a more widespread occurrence. This class is characterised by the presence of a catalytic Ni–Fe binuclear active site, and can be sub-divided into several groups based on sequence alignments, which correlate to distinct physiological functions, subunit composition, and cellular location [10, 12]. The largest and most studied group of [NiFe] Hases is that of the membrane-bound, periplasmic-oriented Hases that oxidise H₂ as an energy source and transfer electrons to the quinone pool through a membrane-bound cytochrome *b* subunit. This group includes the [NiFe] Hases of SRB, even though most of these enzymes are soluble and lack the cytochrome *b* subunit.

Hases from SRB have been extensively studied and have served as models for this type of proteins (for reviews see [8, 13–16]). Hydrogen is a key compound for SRB, since it is one of their major energy sources in natural habitats, and also an intermediate in their energy metabolism, and Hases are generally very abundant in these bacteria. Many species have been shown to have more than one type of Hase (of the [NiFe], [NiFeSe] and [FeFe] groups), but a screening of 25 *Desulfovibrio* (*D.*) spp. showed that only the genes encoding for [NiFe] Hases are always present [17]. Up until recently only the periplasmic-facing Hases of SRB were characterised and these have some unique characteristics: the [NiFe] and [NiFeSe] Hases have the simplest composition, with only the catalytic and electron transferring subunits. These Hases (and also the periplasmic [FeFe] Hase) are unusual in having as electron acceptor a soluble cytochrome *c*, the Type I cytochrome *c*₃ (TpI *c*₃). The TpI *c*₃ then transfers electrons to several other cytochromes *c* in the periplasm of these bacteria, some of which are associated with transmembrane redox complexes that feed electrons for reduction of sulphate in the cytoplasm [13, 18–21]. Another unusual aspect of SRB Hases is that *Desulfovibrio* spp. are the only known organisms to contain a periplasmic [FeFe] Hase. Recently, it was discovered that *Desulfovibrio* spp. may also have a cytoplasmic multi-subunit membrane-bound Hase [22], belonging to the family of Hases that are related to NADH:quinone oxidoreductase (Complex I) [23]. The physiological reason for the apparent redundancy of Hases in SRB is still unclear, as is the exact physiological role of each of them. Double and triple Hase mutants of *D. fructosovorans* failed to display striking physiological differences, suggesting that the loss of one enzyme might be compensated by another and that a fourth Hase is present in this organism [24, 25]. This apparent redun-

dancy contributes to the robustness of these bacteria and shows clearly the importance of Hases in their metabolism.

The recently published genome of *D. vulgaris* Hildenborough (*DvH*) [21] contains genes encoding for six different Hases: two [NiFe] isoenzymes, one [NiFeSe] Hase, and one [FeFe] Hase, all of which are periplasmic or membrane-associated facing the periplasm, and two multi-subunit membrane-bound [NiFe] Hases facing the cytoplasm. This makes *DvH* an excellent model to study the role of Hases in *Desulfovibrio*. The *DvH* [FeFe] Hase has an extremely high H₂-uptake activity, and studies with a mutant lacking this Hase indicate that its physiological role is indeed hydrogen uptake with both H₂ or lactate as electron donors for sulphate reduction [26]. The [NiFe] Hase isoenzyme 1 ([NiFe]₁) from *DvH* has similar characteristics to other *Desulfovibrio* [NiFe] enzymes [27], but it is unusually associated with the membrane, even though its sequence has no predicted transmembrane helices and it lacks the cytochrome *b* subunit. A similar membrane association was reported for a [NiFeSe] Hase in this organism [28]. The *DvH* [FeFe] and [NiFe]₁ Hases both have the TpI *c*₃ as their physiological partner [19, 29].

Studies on [NiFeSe] Hases from SRB have focused on enzymes from *Desulfomicrobium* (*Dm.*) spp. [30, 31]. Sequence analysis of the *Dm.* [NiFeSe] Hases shows that these belong to the large family of the [NiFe] Hases [32]. The [NiFeSe] Hases have some distinctive and very interesting properties, including a higher activity when compared to [NiFe] Hases [33, 34], as well as an apparent resistance to inactivation by oxygen, being isolated aerobically in a catalytically competent state [31]. Furthermore, the H₂/HD ratio measured in the D₂-H⁺ exchange reaction seems to be very different in the [NiFeSe] from the [NiFe] Hases [31]. These differences have been attributed to the presence of selenium in the form of selenocysteine (SeCys), shown by EPR and EXAFS to be a direct ligand to the active-site nickel [33, 35]. This was later confirmed by determination of the crystal structure of the reduced enzyme from *Dm. baculatum* [36]. Two [NiFeSe] Hases from the methanogenic organism *Methanococcus voltae* have also been investigated in detail [37, 38]. In this work we describe a detailed characterisation of the [NiFeSe] Hase isolated from the membranes of *DvH*, aimed at understanding the physiological role of this enzyme in SRB metabolism and at analysing the relationship between its sequence and structural characteristics and its interesting catalytic properties.

Materials and methods

Cell growth and preparation of the membrane extract

Desulfovibrio vulgaris Hildenborough (DSM 644) was grown in lactate/sulphate medium as previously described [39]. The preparation of the membrane extract

was performed as in [20]. The membranes were washed twice with 10 mM Tris-HCl buffer, pH 7.6, to remove soluble and weakly bound proteins, and membrane proteins were extracted by homogenising twice the membrane pellet in 20 mM Tris-HCl buffer, pH 7.6, with 2% (w/v) Zwittergent 3-12 (*N*-dodecyl-*N,N*-dimethyl-3-ammonio-1-propanesulphonate), followed by centrifugation at 140,000× *g* for 1 h.

Protein purification

All purification procedures were performed at a pH of 7.6 and at 4°C, and in the presence of 0.2% (w/v) Zwittergent 3-12, except for the soluble form of the [NiFeSe] Hase ([NiFeSe]_s). The detergent extract was loaded on a DEAE Sepharose Fast Flow column (Pharmacia, 5×40 cm) equilibrated with 20 mM Tris-HCl buffer, and a linear gradient of 0–400 mM NaCl (2.4 l) in the same buffer was applied. The fraction eluted at around 300 mM NaCl with Hase activity was concentrated by ultrafiltration and dialysed to lower the ionic strength. This fraction was then passed on a Pharmacia Q-Sepharose HP column (Hiload 26/10, flow rate 5 ml/min) equilibrated with 50 mM Tris-HCl, and eluted with a stepwise gradient of NaCl. The fraction eluted at 350 mM NaCl was concentrated, and the membrane-bound [NiFeSe] Hase ([NiFeSe]_m) was finally purified on a Superdex 200 column equilibrated and eluted with 100 mM Tris-HCl, 100 mM NaCl (flow rate 1.5 ml/min). This column yielded pure [NiFeSe]_mHase as judged by the SDS-PAGE and activity-stained native gel.

For purification of the [NiFeSe]_s form of the Hase the low ionic strength extract obtained by washing the crude membranes was loaded on a DEAE Sepharose Fast Flow column (Pharmacia, 5×40 cm) equilibrated with 5 mM Tris-HCl buffer without detergent, and a linear gradient of 0–400 mM NaCl (2.4 l) in the same buffer was applied. The fraction eluted at around 300 mM NaCl was concentrated by ultrafiltration and dialysed to lower the ionic strength. This fraction was then passed on a Pharmacia Q-Sepharose HP column (Hiload 26/10) equilibrated with 5 mM Tris-HCl, and eluted with a stepwise gradient of NaCl. The fraction eluted at 250 mM NaCl was concentrated, dialysed and loaded on a ceramic HTP column (15×2.6 cm) equilibrated with 10 mM phosphate buffer, and a stepwise gradient with 1 M phosphate was applied. The fraction eluted at 300 mM phosphate was finally purified by passage on a Superdex 200 column equilibrated and eluted with 50 mM Tris-HCl, 100 mM NaCl. This column yielded pure [NiFeSe]_s Hase as judged by the SDS-PAGE and activity-stained native gel.

Analytical methods

Protein concentration was determined with the Bicinchoninic Acid assay from Pierce, using bovine serum

albumin as the standard. Metal content was determined by inductively coupled plasma emission analysis. Protein molecular masses were determined by 12% SDS-PAGE using BioRad low-range protein standards. H₂-uptake activity in native gels was detected as described [40], with some modifications. The native PAGE was performed on a 10% gel containing 0.1% Triton X-100, under aerobic conditions. The running buffer also contained 0.1% Triton X-100. The gel was placed in a 50 mM Tris-HCl, pH 8, 0.5 mM methyl viologen (MV) solution and deaerated with argon, followed by incubation under a H₂ atmosphere. A 1% 2,3,5-triphenyltetrazolium chloride solution was used to fix the bands. For glycoprotein detection SDS-PAGE gels were fixed with 12.5% trichloroacetic acid and stained with Alcian Blue [41]. The N-terminal sequence was determined by the method of Edman and Begg using an Applied Biosystems 491 HT sequencer.

Spectroscopic methods

UV-Vis spectra were recorded on a Shimadzu UV-1603 spectrophotometer. EPR spectra were recorded using a Bruker ESP 380 spectrometer equipped with an ESR 900 continuous-flow helium cryostat (Oxford Instruments), as previously described [42].

Mass spectrometry methods

Mass spectra of intact proteins and tryptic peptides were assayed in a Voyager-DE STR (Applied Biosystems) matrix-assisted laser desorption ionisation time-of-flight (MALDI-TOF) mass spectrometer. Hases large-subunit bands were excised from SDS-PAGE and polypeptides subjected to reduction, alkylation and digestion with sequencing-grade modified trypsin (Promega) according to Pandey et al. [43]. Peptide co-crystallisation was achieved by applying 0.5 µl of the sample on plate and adding on top equal volume of recrystallised matrix α -cyano-4-hydroxycinnamic acid (CHCA) (10 mg/ml) prepared in acetonitrile (50%, v/v) with trifluoroacetic acid (0.1%, v/v). The same cocrystallisation procedure was used for the intact Hases, but in this case the matrix was sinapinic acid. The mixture was allowed to air dry (dried droplet method). Monoisotopic tryptic peptide masses were used to search for homologies and protein identification with Peptide Mass Fingerprint of Mascot (<http://www.matrixscience.com>). Searches were done in the MSDB database. A mass accuracy of 50–100 ppm was considered for external calibrations and Cys carbamidomethylation and Met oxidation were considered as fixed and variable amino-acid modifications, respectively. Criteria used to accept the identification were significant homology scores achieved in Mascot [44], and a minimum of four peptides matches, allowing protein sequence coverage superior to 10%.

Enzymatic activities

The hydrogen production activity was determined by gas chromatography, at pH 7.0, as described in [45] with dithionite as the electron donor in the presence of MV; H₂-uptake activity was determined spectrophotometrically at 25°C in anaerobic cuvettes using benzyl viologen (BV) as the electron acceptor [46]. All experiments were performed at least in triplicate. One unit of Hase activity is defined as 1 μmol of H₂ produced or consumed per minute. To study the effect of phospholipids or detergent on the H₂ production activity the Hases were diluted in parallel for the activity assays in either 20 mM Tris-HCl buffer, pH 7.6, or the same buffer containing 0.2% Zwittergent 3-12 or a phospholipid mixture at 12 mg/ml. The phospholipid mixture contained 5% Cardiolipin (0.6 mg/ml), 20% L-Phosphatidyl glycerol (2.4 mg/ml) and 75% Phosphatidyl ethanolamine (9 mg/ml) (all phospholipids were from Sigma) and was prepared in 20 mM Tris-HCl, pH 7.6, in two steps: the organic solutions of the phospholipids were mixed and the solvents were removed using a Speed Vacuum Plus SC110A Savant apparatus; then the mixture was rehydrated in 20 mM Tris-HCl, pH 7.6 (with a final concentration of 12 mg/ml), and homogenised by sonication as previously described [47]. The homogeneous phospholipid mixture was incubated for 10 min in ice and then used for dilution of the Hases as described [47]. The Hases were diluted in parallel (1,000× for the [NiFeSe]_m and [NiFe]₁ Hases, and 500× for the [NiFeSe]_s) in the three conditions studied, and after the 20 min incubation on ice 10 μl of the final dilution was used in a 1 ml reaction mixture.

Hydrogen production activity with reduced cytochromes as electron donors was also determined by gas chromatography, in 100 mM Tris-HCl, pH 7.6, 15 mM dithionite and 0.0001% rezazurin. The concentrations used were TpI c₃/[NiFe]₁ Hase: 4 μM TpI c₃, 0.2 μM [NiFe]₁ Hase; TpII c₃/[NiFe]₁ Hase: 4 μM TpII c₃, 3 μM [NiFe]₁ Hase; TpI c₃/[NiFeSe] Hase: 4 μM TpI c₃, 0.1 μM [NiFeSe] Hase; TpII c₃/[NiFeSe] Hase: 4 μM TpII c₃, 1 μM [NiFeSe] Hase. In control experiments cytochromes were replaced by MV at the following concentrations—MV/[NiFe]₁ Hase: 4 μM MV, 0.1 μM [NiFe]₁ Hase; MV/[NiFeSe] Hase: 4 μM MV, 0.2 μM [NiFeSe] Hase. H₂ production from dithionite alone was negligible for both Hases.

The reduction of *DvH* periplasmic cytochromes TpI c₃, TpII c₃ and high molecular mass cytochrome (HmcA) with [NiFeSe] Hase was performed in a stirred cell, with a hydrogen overpressure of 15 kPa flowing through the cell, and followed with a Shimadzu UV3100 spectrophotometer. The buffer used in all cases was 100 mM Tris-HCl (pH 7.6). The reduction of the cytochromes was measured by following the increase in absorption at 553 nm for TpI c₃, 551 nm for TpII c₃ and at 552.5 nm for HmcA, using the respective absorption coefficients. The rates were

measured from the initial linear segment of the reduction curves. The concentrations used were chosen so that a reasonable rate could be measured, after having assured that the rates were proportional to the Hase concentrations. Each of the experiments, performed as previously described [19], was repeated at least three times. The concentrations used were TpI c₃/Hase: 4 μM TpI c₃ and 14 nM Hase; HmcA/Hase: 1 μM HmcA and 0.13 μM Hase; HmcA/Hase/TpI c₃: 1 μM HmcA, 0.13 μM Hase and 0.13 μM TpI c₃.

Sequence analysis tools

Sequence data were retrieved and analysed at The Institute for Genomic Research website (<http://www.tigr.org>), at the DOE Joint Genome Institute website (http://www.jgi.doe.gov/JGI_microbial/html/index.html) and the VIMSS Comparative Genomics website (<http://www.microbesonline.org/>). Multiple alignments were performed using CLUSTAL X.

Structure modelling

Since there is no three dimensional structure determined for the [NiFeSe] Hase from *DvH*, a comparative model was built based on its sequence and the structures available in the Protein Data Bank. Both the large and the small subunits of the Hase were modelled based on the two subunits of the [NiFeSe] Hase from *Dm. baculatum* [36] (PDB entry 1CC1 [36]), which are the ones with the higher sequence homology (67% for the large subunit and 60% for the small subunit) with the target, among all the available structures in the database. Due to the high sequence identity we can be sure that a good structural model is obtained [48, 49].

The program MODELLER [50], Version 6.1, was used for deriving the structure. The alignment was optimised through several modelling cycles until a good quality model for the unknown structure was achieved. The quality was assessed by considering the restraint violations reported by MODELLER [50] and a Ramachandran analysis performed by the program PROCHECK [51]. The final model has 92.7% of the residues in the most favoured regions, and 7.0% in additional allowed regions. There were only two residues in the disallowed regions, which correspond to equivalent residues in the X-ray structure used as the basis for this comparative modelling.

Internal water molecules were also modelled together with the structure. From the 329 crystallographic water molecules in the template, we selected the ones that established at least two hydrogen bonds with the protein residues in the template structure and that were compatible with the target. 159 internal water molecules were modelled.

Results and discussion

Purification and molecular characteristics

D. vulgaris Hildenborough cells grown in lactate/sulphate medium exhibit a high level of Hase activity associated with the membranes, and we were interested in isolating the Hase(s) responsible for this activity. The *DvH* genome sequence reveals the presence of two cytoplasmic-facing, multi-subunit membrane-bound Hases including one similar to the *Methanosarcina barkeri* Ech Hase [52], also present in *D. gigas* (*Dg*) [22], and one similar to the CO-induced Hase of *Rhodospirillum rubrum* [53]. Two [NiFe] and one [NiFeSe] Hase had previously been detected in the membranes of *DvH* [28]. One of these [NiFe] Hases was purified and characterised by us [27], and corresponds to the bicistronic [NiFe]₁. At that time a second, more acidic, major peak with Hase activity was described upon purification of the membrane extract. Here we report the purification of the Hase present in this second peak, which yielded a protein with two subunits of 63 and 35 kDa by SDS-PAGE (Fig. 1, lane 1). N-terminal sequence analysis of the small subunit permitted identification of this Hase from the genome sequence as the [NiFeSe] Hase (the large subunit had a blocked N-terminal). The sequence-predicted molecular masses of the two subunits, including cofactors, are 54.4 and 31.4 kDa. The Ech and CO-induced Hases of *DvH* were not detected during purification of the membrane extract. This could be due to the intrinsic instability of these Hases, a characteristic of the family of multi-subunit membrane [NiFe] Hases related to Complex I [23], or to a low level of expression [54].

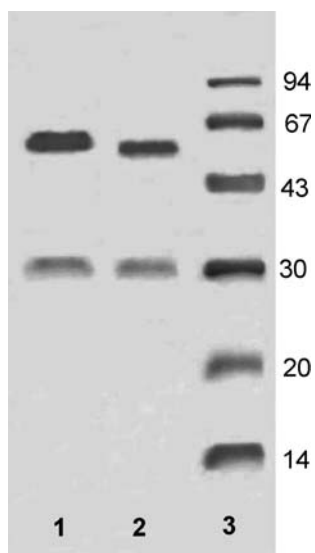


Fig. 1 12.5% SDS-PAGE, stained with Coomassie Blue. (1) *DvH* [NiFeSe]_mHase; (2) *DvH* [NiFeSe]_sHase; (3) molecular mass markers

The UV-Vis spectrum of the [NiFeSe] Hase (not shown) is very similar to that of the [NiFe]₁ Hase and shows the characteristic broad absorption centred at 400 nm due to the oxidised FeS centres, and a A_{280}/A_{400} ratio of 4.43. Chemical analysis of the isolated Hase confirmed the presence of selenium in equimolar amounts to nickel (ratio Ni:Se:Fe of 1:1:15).

The [NiFeSe] Hase purified from the membranes ([NiFeSe]_m) displays a very high catalytic activity when compared to the other [NiFe] Hases, like the *DvH* [NiFe]₁ or the *Dg* [NiFe] Hase, (Table 1), particularly in H₂ production from MV which is even higher than that of the periplasmic *DvH* [FeFe] Hase. The activity of the *DvH* [NiFeSe]_m Hase is very sensitive to the presence of detergent or phospholipids. If the enzyme is diluted in buffer without detergent the activity becomes erratic and is considerably reduced (see below). Similar high H₂ production values have been reported for the [NiFeSe] Hases from *Dm. baculatum* DSM 1743 [33] and *Dm. baculatum* New Jersey [34]. However, this should not be taken as evidence that the [NiFeSe] Hases physiological function is H₂ production since this activity was measured with an artificial electron donor (MV), whereas with a physiological electron donor (TpI *c*₃) the H₂ production activity of the [NiFeSe]_m Hase is of the same order of magnitude as that of the [NiFe]₁ Hase (see below). It seems likely that the low activities reported for the *DvH* [NiFe]₁ Hase are due to the fact that it is isolated in an inactive form containing Ni(III) (a mixture of Ni-A and Ni-B states), whereas the [NiFeSe]_m is in an active Ni(II) state. Recently, it has also been shown that the activity of [NiFe] Hases, measured by conventional assays, is probably much lower than their real activity since when the enzymes are adsorbed on an electrode H₂ oxidation occurs at a diffusion-controlled rate ([5] and references therein).

The soluble form of the [NiFeSe] Hase

In an aged preparation of the [NiFeSe]_m Hase, judged to be pure by SDS gel, a second band of unknown origin (named as X) was detected in a native gel stained for Hase activity (Fig. 2, lane 5). This second band did not correspond to the [FeFe], [NiFe]₁ or native membrane-bound form of the [NiFeSe] Hase ([NiFeSe]_m). This band was extracted from the gel, denatured by treatment with SDS and run on a SDS-PAGE gel, displaying the two characteristic Hase subunits (Fig. 1, lane 2). However, a careful analysis reveals that the [NiFeSe]_m large subunit has a slightly higher molecular mass than the X large subunit. The N-terminal of the [NiFeSe]_m Hase large subunit is blocked whereas that of the X large subunit gave the sequence (GATGR) which corresponds to the sequence of the [NiFeSe] Hase large subunit from residue 12. The N-terminal sequences of the small subunits from [NiFeSe]_m and X are identical. This shows that X is a form of the [NiFeSe] Hase (named as [NiFeSe]_s since it was subsequently found to be soluble),

Table 1 Catalytic activities of Hases (in U/mg)

	<i>DvH</i> [NiFeSe] Hase	<i>DvH</i> [NiFe] ₁ Hase	<i>DvH</i> [FeFe] Hase	<i>Dg</i> [NiFe] Hase	<i>Dmb</i> [NiFeSe] Hase	<i>Dmb</i> NJ [NiFeSe] Hase
H ₂ production	6,908	174	4,800	440	2,000	8,600
H ₂ consumption	900	89	50,000	1,500	—	—

Data are from [14] for *DvH* [FeFe] and *D. gigas* [NiFe] Hases, from [27] for *DvH* [NiFe]₁ Hase, from [33] for *Dm. baculatum* DSM 1743 [NiFeSe] Hase and [34] for *Dm. baculatum* New Jersey [NiFeSe] Hase

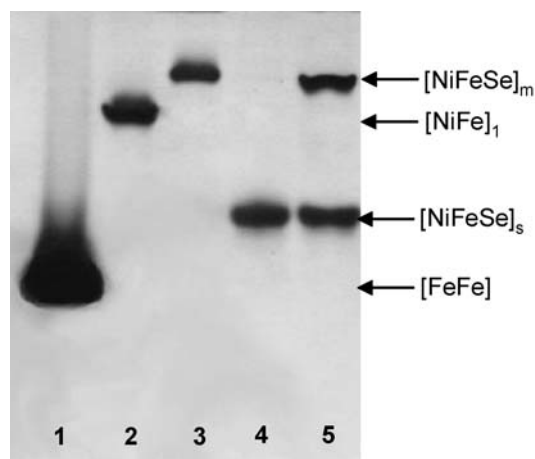


Fig. 2 Activity-stained native PAGE. 1 *DvH* [FeFe] Hase; 2 *DvH* [NiFe]₁ Hase; 3 *DvH* [NiFeSe]_m Hase; 4 *DvH* [NiFeSe]_s Hase; 5 *DvH* [NiFeSe]_m fraction containing some [NiFeSe]_s as a degradation product

different from the [NiFeSe]_m. Both the [NiFeSe]_m and [NiFeSe]_s proteins were negative in a gel stained to detect glycoproteins, and no glycosylation sites were identified through the sequence.

When crude cell extracts were analysed by activity gel it was observed that the soluble extract contained mainly the [FeFe] Hase, the membrane extract contained mainly

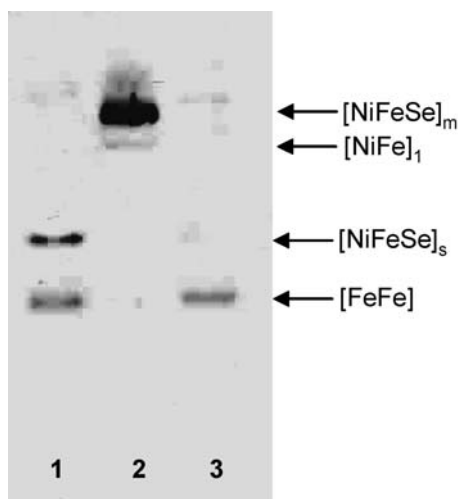


Fig. 3 Activity-stained native PAGE. 1 Low ionic strength extract of membrane fraction; 2 Detergent extract of membrane fraction; 3 soluble fraction

the [NiFeSe]_m Hase, whereas an extract obtained by washing the membranes with low ionic strength buffer contained the [FeFe] Hase and the [NiFeSe]_s Hase (Fig. 3). It was also observed that some fractions which contained only the [NiFeSe]_m Hase at the early stages of purification later developed the X band, suggesting that the [NiFeSe]_m Hase could generate the [NiFeSe]_s form. However, it was possible to isolate the pure forms of the [NiFeSe]_m and [NiFeSe]_s Hase, using a fast purification protocol, from the membrane detergent extract and low ionic strength extract, respectively.

It is noteworthy that the [NiFeSe]_m remains associated with the membranes upon suspension in a low ionic strength buffer, but not the [NiFeSe]_s (Fig. 3). In addition, the two forms seem to differ in the N-terminal of the large subunit, and they run very differently on a native gel. One likely explanation for these observations would be the presence of a hydrophobic group (e.g. a lipid) added post-translationally to the N-terminal of the [NiFeSe] Hase which would be responsible for the association of the [NiFeSe]_m form with the membranes and its requirement for detergent, and would prevent its N-terminal sequencing. Cleavage of this hydrophobic group would result in formation of the [NiFeSe]_s form which is soluble and does not have a blocked N-terminal. A similar situation could be responsible for the reported, and thus far unexplained, membrane association of the *DvH* [NiFe]₁ Hase [27] and *D. vulgaris* Miyazaki [NiFe] Hase [29]. Interestingly, the three Hases (and the ones in *D. desulfuricans* G20) share a conserved N-terminal sequence of about ten residues that is absent in other *Desulfovibrio* periplasmic [NiFe] Hases that do not associate with the membranes (Fig. 4). The conserved Gly12 is the first amino-acid detected in the [NiFeSe]_s N-terminal. This N-terminal sequence does not display a typical prokaryotic lipoprotein sequence for processing and attachment of a glyceride-fatty acid lipid to a cysteine [55], but does have a conserved cysteine in the fourth position which could possibly be involved in such a process.

Mass spectrometry (MALDI-TOF) of the [NiFeSe]_m Hase reveals a molecular mass of 54,820 Da for the large subunit, which is higher by 418 Da than that predicted from the total amino-acid sequence including all cofactors. It is not possible to calculate the actual mass of the [NiFeSe]_m Hase large subunit due to the probable post-translational modification of the N-terminal, which may include removal of an uncertain number of residues. However, the difference in mass observed is in a range

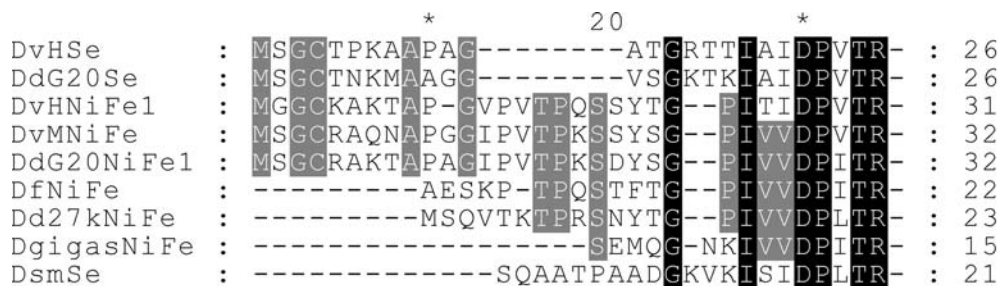


Fig. 4 Sequence alignment of the N-terminal region of several *Desulfovibrionaceae* Hases. *DvHSe* *D. vulgaris* Hildenborough [NiFeSe]_s Hase; *D20Se* *D. desulfuricans* G20 [NiFeSe]_s Hase; *DvHNiFe1* *D. vulgaris* Hildenborough [NiFe]₁ Hase; *DvMNiFe* *D. vulgaris* Myizaki [NiFe]₁ Hase; *DdG20NiFe1*- *D. desulfuricans*

G20 [NiFe]₁ Hase; *DfNiFe* *D. fairfieldensis* [NiFe] Hase; *Dd27kNiFe* *D. desulfuricans* 27774 [NiFe] Hase; *DgigasNiFe* *D. gigas* [NiFe] Hase; *DsmSe* *Dm. baculatum* [NiFeSe]_s Hase. Strictly conserved residues are in the *black background*, and partially conserved residues in the *grey background*

that agrees with the addition of a group such as a diacyl glyceride, as observed in some lipoproteins. For the [NiFeSe]_s Hase a molecular mass of 53,082 was obtained for the large subunit, which is lower by 309 Da than that predicted from the sequence without the first 11 residues. We also analysed peptides obtained by the tryptic digestion of the [NiFeSe]_m and [NiFeSe]_s large subunits. The identified peptides correspond to a coverage of 62% of the complete amino-acid sequence predicted for the [NiFeSe]_m Hase. The only difference observed between the two MALDI-TOF spectra is a peak at 771.4 Da corresponding to peptide 8–16, which is present only in the tryptic digest of the membrane-bound form. This supports the previous observation that the difference between soluble and membrane-bound forms of the [NiFeSe] Hase is located in the N-terminal. Furthermore, it indicates that residue 8 is present in the [NiFeSe]_m form, whereas the [NiFeSe]_s sequence starts with Gly12. Further studies are underway to elucidate the nature of the apparent post-translational modification of the [NiFeSe]_m Hase.

The considerable difference in migration on a native gel between the [NiFeSe]_m and [NiFeSe]_s forms is most likely due to the effect of the hydrophobic group at the N-terminal of the [NiFeSe]_m Hase. The possibility that this difference could be due to the aggregation of the [NiFeSe]_m form seems unlikely because the native gels were run in the presence of detergent. It was observed that if the detergent is not added the Hases do not run properly in the native gel (they are retained in the stacking gel as detected by activity staining) and only streaking is observed, which is highly suggestive that

aggregation does occur in the absence of detergent. The fact that detergent prevents this streaking and leads to the formation of well resolved bands suggests that aggregation is prevented in the conditions used.

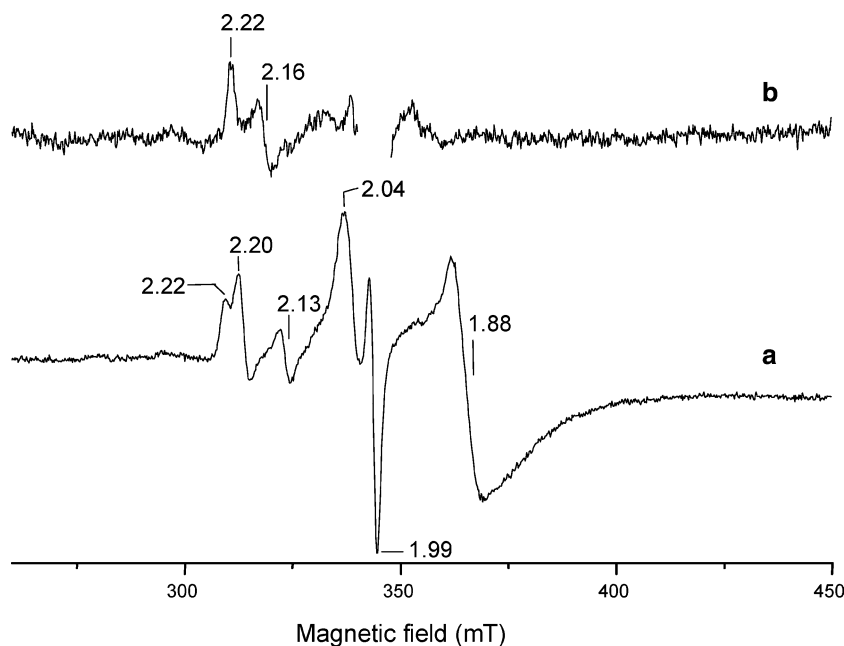
Based on the assumption that there is a lipid group in the [NiFeSe]_m Hase, we studied the effect of the detergent and phospholipids on the activity of this and the [NiFeSe]_s and [NiFe]₁ Hases. A phospholipid mixture was prepared to mimic the phospholipid composition of *DvH* membranes [56], containing 5% Cardiolipin, 20% L-Phosphatidylglycerol and 75% Phosphatidylethanolamine. The three Hases display higher activities in the presence of phospholipids (Table 2). [NiFeSe]_m is the most sensitive to the hydrophobicity of the medium, having 70% of the maximum activity in the presence of detergent instead of phospholipids, and only 40% in the absence of either phospholipids or detergent. In contrast, the [NiFeSe]_s form had considerably less activity than the [NiFeSe]_m (8%) but was relatively insensitive to the hydrophobicity of the medium with 97% of the activity in the presence of detergent and retaining 80% in the absence of either phospholipids or detergent. These results support the idea that the [NiFeSe]_m Hase contains a hydrophobic group which is important for its activity and is not present in the [NiFeSe]_s form, which presents a much reduced activity in all conditions tested. The presence of phospholipids probably induces a proper configuration for the hydrophobic group resulting in higher activity. The effect of phospholipids seems to be specific since there is still a 30% difference relative to the activity in the presence of detergent, which should already eliminate unspecific effects like aggregation.

Table 2 H₂ production activity (U/mg) of *DvH* [NiFeSe]_m, [NiFeSe]_s and [NiFe]₁ Hases diluted in the presence of Tris-HCl buffer, Tris-HCl buffer with 0.2% Zwittergent 3–12 or Tris-HCl buffer with phospholipids

	Phospholipids	0.2% Zwittergent 3–12	Tris-HCl buffer
[NiFeSe] _m Hase	6,908 (100%)	4,787 (70%)	2,755 (40%)
[NiFeSe] _s Hase	580 (100%)	560 (97%)	460 (80%)
[NiFe] ₁ Hase	495 (100%)	441 (90%)	366 (74%)

The values in percentage are relative to the activity determined in the presence of phospholipids

Fig. 5 EPR spectrum of the H₂-reduced *DvH* [NiFeSe]_m Hase. **a** 6.5 K; **b** 20 K; microwave frequency 9.64GHz, microwave power 2.4 mW, modulation amplitude 1 mT



The *DvH* [NiFe]₁ Hase is also associated with the membranes but displays less sensitivity to the presence of phospholipids or detergent than the [NiFeSe]_m Hase.

EPR studies

The isolated oxidised *DvH* [NiFeSe]_m Hase is in an EPR-silent state as reported for other [NiFeSe] Hases [30, 31]. This indicates that the enzyme is in a Ni(II) state contrary to most oxidised [NiFe] Hases which are in an inactive Ni(III) state containing either a bridging hydroxo or hydro-peroxide ligand between the Ni and the Fe ions at the binuclear centre [57]. A signal corresponding to a [3Fe4S]¹⁺ centre is not observed, even after oxidation of the enzyme with ferricyanide, which agrees with the sequence-based prediction that the medial cluster is a [4Fe4S]^{2+/1+} centre and not a [3Fe4S]^{+1/0} one as observed in most H₂-uptake [NiFe] Hases.

After reduction with H₂ several resonances develop, due to the nickel ion and to the reduced [4Fe4S]¹⁺ centres (Fig. 5). The resonances with $g_{\max} \sim 2.04$ and $g_{\text{med, min}} \sim 1.88$ are due to the FeS centres, which are fast relaxing and are no longer detected at 20 K. At a lower magnetic field resonances at $g = 2.22$, 2.20 and 2.13 are due to the nickel ion in the 3+ oxidation state (the so-called Ni-C state) in magnetic interaction with the nearby $S = 1/2$ reduced [4Fe4S]¹⁺ cluster. At higher temperature this interaction vanishes and a single rhombic species with $g = 2.22$, 2.16 and 2.0 (not seen due to overlap with the radical signal) is observed. Upon re-oxidation in air of the reduced [NiFeSe]_m Hase the EPR-silent state is obtained, confirming that the enzyme is resistant to the formation of the inactive Ni-A/Ni-B

species. The soluble [NiFeSe]_s Hase displayed identical EPR properties to the membrane-bound form.

Reduction of periplasmic cytochromes by the [NiFeSe] Hase

Periplasmic-facing Hases from SRB are unusual in having as electron acceptor a soluble cytochrome *c* (TpI *c*₃) rather than a membrane-bound haem *b* cytochrome which interacts directly with the quinone pool. Interestingly, the same situation holds for the formate dehydrogenases isolated from these organisms [21, 58, 59]. SRB are characterised by expressing several periplasmic multi-haem cytochromes *c*, which can receive electrons from TpI *c*₃ [19, 20, 60–62]. The genome of *DvH* encodes for an even higher number of periplasmic cytochromes *c* than previously considered. These cytochromes probably constitute a network of interconnecting electron transfer pathways that will feed electrons to the cytochromes *c* associated with membrane complexes. The [NiFeSe] Hase operon also lacks the gene for a haem *b* cytochrome, so its natural partner is most likely also a cytochrome *c*. The difference between the periplasmic-facing Hases could be in their physiological electron acceptor, so we tested the reactivity of the [NiFeSe] Hase with the most abundant cytochromes *c* in the periplasm of *DvH*, so far isolated: the TpI *c*₃, the tetra-haem TpII *c*₃ that is associated with a membrane complex [13, 20], and the 16-haem HmcA cytochrome also associated with a membrane complex [63]. The rates of reduction of each cytochrome with the [NiFeSe] and [NiFe]₁ Hases are presented in Table 3. Overall the two Hases display similar reactivity, with the TpI *c*₃ being the preferred electron acceptor. The TpII *c*₃ is also reduced with a

Table 3 Rates of reduction of *DvH* periplasmic cytochromes with Hases (U/mg)

	[NiFeSe] _m Hase	[NiFe] ₁ Hase
TpI <i>c</i> ₃	25.6	36.8
TpII <i>c</i> ₃	8.0	4.6
TpII <i>c</i> ₃ + TpI <i>c</i> ₃	17.4	17.4
HmcA	0.024	0.032
HmcA + TpI <i>c</i> ₃	1.6	0.64

lower, but significant rate, whereas direct reduction of HmcA by either Hase is very slow. The reduction of the TpII *c*₃ and HmcA by the [NiFeSe] Hase is faster in the presence of catalytic amounts of the TpI *c*₃, as is also observed with the [NiFe]₁ and [FeFe] Hases [19]. Given that the TpI *c*₃ is also much more abundant in cells of *DvH* than other cytochromes, we can conclude that this cytochrome is the physiological partner for the [NiFeSe] Hase as well as for the [NiFe]₁ and [FeFe] Hases.

It is noteworthy that the second [NiFe] Hase isoenzyme of *DvH* ([NiFe]₂) probably has a different cytochrome as electron acceptor since its genes are encoded in the same locus as a gene coding for a TpI *c*₃ homologue (and the same is observed in the genome of *DdG20*). Sequence analysis indicates that this cytochrome is related to the dimeric cytochromes *c*₃ (also called cytochrome *c*₃ 26,000) which have been isolated from *D. gigas* [64], *Dm. norvegicum* [65] and *D. africanus* [60]. In *DvH*, the dimeric cytochrome *c*₃ and the [NiFe] Hase 2 were never reported suggesting they may be expressed in different conditions than those commonly used to grow this organism.

We tested also the H₂ production activity of the [NiFeSe] and [NiFe]₁ Hases with the dithionite-reduced cytochromes as electron donors. These experiments are possible because the activity of either Hase with dithionite alone is negligible. For comparison we measured the activity with MV at the same concentration as used with the cytochromes (4 μM). The [NiFeSe] Hase displays a H₂ production activity with the TpI *c*₃ (5.3 U/mg) that is two times higher than that observed with MV at the same concentration (2.5 U/mg), whereas both activities are of the same order in the case of the [NiFe]₁ Hase (8.2 versus 8.6, respectively). In contrast, the TpII *c*₃ is a poor electron donor for both Hases (0.2 U/mg in both cases) in agreement with its role as an electron donor to the membrane associated redox complex. With their physiological redox partner (TpI *c*₃) the [NiFeSe] and [NiFe]₁ Hases display a higher activity in H₂ oxidation than in H₂ production. However, the two activities are not largely different suggesting that both Hases may function bidirectionally in vivo, if, for example, it is necessary for the cell to dispose of excess reducing power. These results indicate a similar reactivity for the [NiFeSe] and [NiFe]₁ Hases, suggesting that both can perform the same physiological function in the cells of *DvH*.

[NiFeSe] Hase sequence analysis

The genes coding for the *DvH* [NiFeSe] Hase large and small subunits are encoded by a putative simple bicistronic operon. There is no adjacent gene coding for a membrane-bound *b* cytochrome, and accordingly the small subunit lacks the C-terminal membrane anchor present in the periplasmic-facing membrane-bound [NiFe] Hases. Furthermore, the sequences of the [NiFeSe] Hase large and small subunits do not include any predicted transmembrane helices or amphipatic helices that could explain the membrane attachment of this Hase, and the same is true for the *DvH* [NiFe]₁ Hase.

The gene for the small subunit of the [NiFeSe] Hase includes a twin-arginine signal peptide of 34 residues, indicating that this Hase is exported to the periplasmic side of the membrane. This contradicts the previously held idea that the [NiFeSe] Hase of *DvH* was facing the cytoplasm [66], which was apparently supported by immunoelectron microscopy experiments [67]. However, in these experiments the cytoplasmic location of the [NiFeSe] Hase was based on the labelling of membrane fragments obtained after passage through a French pressure cell, which is known to generate inverted membrane vesicles, thus misleading the conclusions. As such, the physiological role of the *DvH* [NiFeSe] cannot be that of cytoplasmic H₂ production in the hydrogen cycling theory for energy coupling in SRB [9]. The periplasmic location suggests that the [NiFeSe] Hase has a role similar to that of the periplasmic [FeFe] and [NiFe]₁ Hases i.e. in H₂ uptake, since H₂ production in the periplasm would be energetically unfavourable.

The genome of *D. desulfuricans* G20 (*DdG20*) (available at <http://www.jgi.doe.gov>) encodes also for a [NiFeSe] Hase very similar to that of *DvH*. The genetic organisation of the locus containing the [NiFeSe] genes is similar in both organisms (Fig. 6). The *hysAB* genes coding for the [NiFeSe] subunits are followed by a *hynC* gene encoding for a C-terminal peptidase [68] which is probably specific for this Hase. Interestingly, the *hynC* gene is followed by the *hynBA-1* genes coding for the [NiFe]₁ subunits, suggesting that there may be some sort of coordinated regulation of the two Hases. The next three genes are predicted to form an operon [69] and include a *hupD/hynC* gene coding for a C-terminal peptidase probably specific for the [NiFe]₁ Hase, a *hynC* gene coding for a chaperone for maturation of a Hase large subunit [68] and a GDSL-lipase homologous to the *E. coli* periplasmic thioesterase I (TesA) of unknown physiological function [70]. To our knowledge the presence of a lipase in a Hase maturation operon is unprecedented and further supports the proposal that the [NiFeSe] and [NiFe]₁ Hases have a lipid group for membrane anchoring. Hydrolysis of this lipid anchor by the lipase would free the Hase from the membrane (possibly leading to the formation of the soluble [NiFeSe]_s form), which could be advantageous under certain physiological conditions.

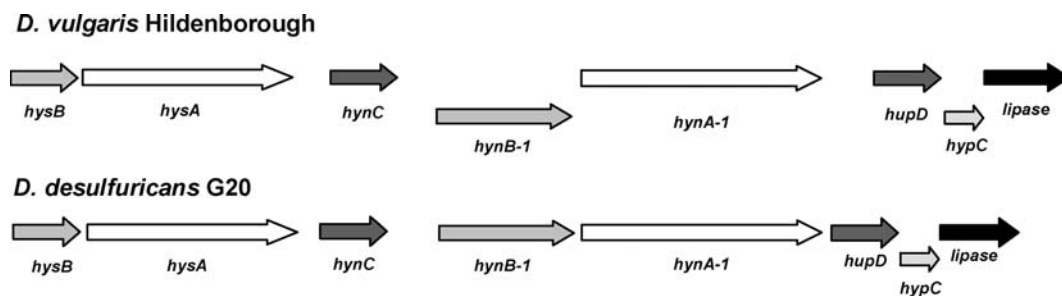


Fig. 6 Schematic representation of the *DvH* and *D. desulfuricans* G20 gene locus containing the [NiFeSe] and [NiFe]₁ Hase genes. Homologous genes have the same colour. *hysAB* [NiFeSe] Hase; *hynA1B1* [NiFe]₁ Hase; *hynC/hupD* C-terminal peptidase; *hycC* maturation chaperone

The *DvH* and *DdG20* [NiFeSe] Hases both have the TGA codon for the SeCys ligand to the nickel, as well as the fourth cysteine ligand to the medial [4Fe4S]^{2+/1+} cluster which is replaced by a proline in most [NiFe] Hases (see Fig. 7d below). This confirms that the presence of three [4Fe4S]^{2+/1+} clusters in the small subunit is a characteristic of the SRB [NiFeSe] Hases, whereas most H₂-uptake [NiFe] Hases have a [3Fe4S]^{1+/0} medial cluster which has a much higher redox potential. The two [NiFeSe] Hases of *M. voltae*, Vhu and Fru, also contain three [4Fe4S]^{2+/1+} clusters. The involvement of the [3Fe4S]^{1+/0} cluster in electron transfer has been questioned due to its high-redox potential, although this may not prevent fast electron tunnelling due to the proximity of the [4Fe4S]^{2+/1+} clusters [71]. Nevertheless, it is intriguing why throughout evolution the group of [NiFeSe] Hases has retained a medial [4Fe4S]^{2+/1+} cluster and most [NiFe] Hases a [3Fe4S]^{1+/0} cluster. This question was addressed with mutant protein studies with opposing results. A mutant of the [NiFeSe] F₄₂₀-reducing Hase (Fru) from *M. voltae* containing a [3Fe4S]^{1+/0} instead of a [4Fe4S]^{2+/1+} cluster displayed a 60% higher H₂ oxidation activity with BV as the electron acceptor, relative to the wild-type protein, but this activity was greatly reduced with the natural electron acceptor F₄₂₀ (7% of the wild-type) [72]. In contrast, a mutant of the *D. fructosovorans* [NiFe] Hase with a [4Fe4S]^{2+/1+} instead of a [3Fe4S]^{1+/0} cluster displayed a 60% higher H₂ production activity, but only a slight reduction (38%) in H₂ oxidation with either MV or the physiological electron acceptor Tpl c₃ [73]. This indicates that the change to a higher redox potential [3Fe4S]^{1+/0} cluster affects electron transfer to F₄₂₀ in the Fru Hase, whereas the presence of a [3Fe4S]^{1+/0} or a [4Fe4S]^{2+/1+} cluster seems not to be relevant for electron transfer between SRB Hases and the Tpl c₃, which is in accordance with the [NiFe]₁ and [NiFeSe] Hases having the same natural partner.

An alignment of the sequences available for three [NiFeSe] Hases from the *Desulfovibrionaceae* family reveals that these form a group that is phylogenetically quite distinct from the other [NiFe] Hases present in the same organisms (e.g. the *DvH* [NiFeSe] Hase large subunit displays only 34% identity and 49% similarity to the *DvH* [NiFe]₁ Hase; see supplementary material),

and they are more closely related to the Hases present in *Carboxydotherrmus hydrogeniformans*, *Dehalococcoides ethenogenes* and the SRB *Desulfohalobium psychrophila*. Interestingly, the Hases from these three organisms contain cysteine rather than SeCys as a ligand to the Ni, so they are standard [NiFe] Hases. Their sequence indicates that the medial cluster is a [4Fe4S]^{2+/1+} cluster as in the [NiFeSe] Hases, which is unusual for periplasmic-facing H₂-uptake [NiFe] Hases. There are several conserved differences observed between this group (formed by the *Desulfovibrionaceae* [NiFeSe] Hases and the [NiFe] Hases with a medial [4Fe4S]^{2+/1+} cluster) and the group of *Desulfovibrio* [NiFe] Hases (that have a medial [3Fe4S]^{1+/0} cluster), some of which are in residues that are close to the active site or to the electron transfer pathways (see discussion of the structural model below).

Structural model of the [NiFeSe] Hase

A comparative model for the *DvH* [NiFeSe] Hase was designed based on the two subunits of the [NiFeSe] Hase from *Dm. baculatum* [36]. We compared the model obtained with the structure of the homologous [NiFeSe] Hase from *Dm. baculatum* [36] (PDB entry: 1CC1), and with the structures of [NiFe] Hases from *D. vulgaris* Miyazaki (*DvM*) [74] (PDB entry: 1H2A) and *D. gigas* [75] (PDB entry: 2FRV). For the sake of clarity, Fig. 7 compares the *DvM* [NiFe] Hase and the *DvH* [NiFeSe] Hase (the model derived here), although the highlighted residues and differences can be generalised for the other Hases in each family. We used the suffices “s” and “L” to designate residues in the small and large subunits, respectively.

The overall structure (Fig. 7a) of the [NiFeSe] Hases is very similar to the [NiFe] Hases, but in the case of [NiFeSe] Hases there is an insertion of 11 residues (I180s to A190s in *DvH* [NiFeSe] Hase) in an external loop in the small subunit, facing the outside and making it larger. The other major differences, as predicted from the sequence analysis, are the presence of a medial [4Fe4S]^{2+/1+} centre in the small subunit instead of a [3Fe4S]^{1+/0}, and the presence of a SeCys coordinating the nickel instead of a cysteine in the [NiFe] Hases.

Despite this overall structural conservation between [NiFeSe] and [NiFe] Hases, there are some noteworthy differences in amino-acids that are strictly conserved among each family (see sequence alignment in supplementary material). Some of these differences relate to charged and polar residues around the metal centres that

may thus have an impact in the catalytic activity, and are discussed below. Our analysis of these conserved differences aims to address the question of whether the higher activity displayed by the [NiFeSe] Hases is due only to the effect of selenium, or is also a result of specific amino-acid residues. Quantum chemical studies of

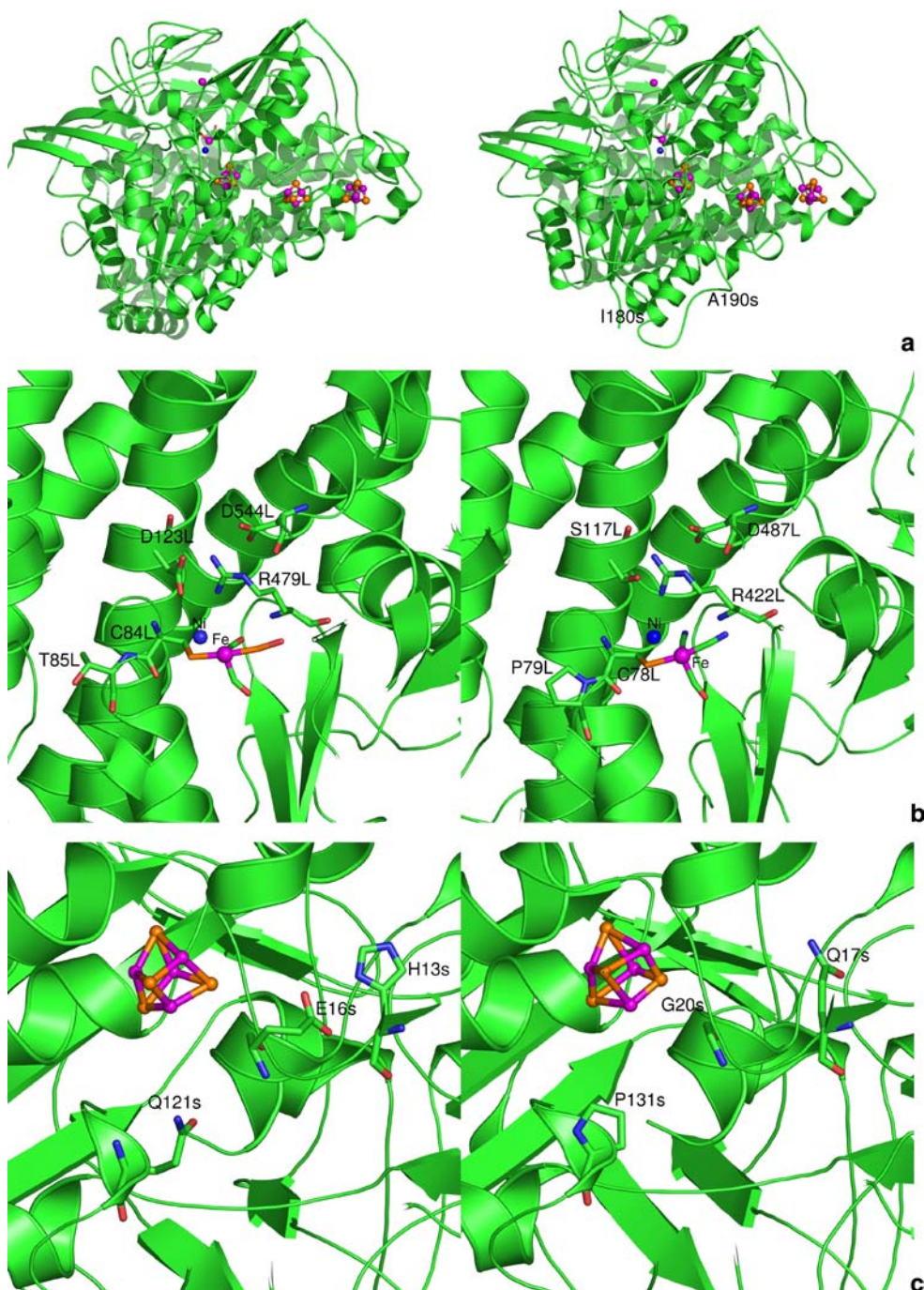


Fig. 7 Comparison between the [NiFe] Hase from *D. vulgaris* Miyazaki (in the left hand side) and the modelled [NiFeSe] Hase from *DvH* (in the right hand side). The proteins are rendered as cartoons, the metal atoms are represented as *small spheres*, the iron ligands are represented as *sticks* and the Fe-S clusters are drawn as *ball and sticks*. In the residue labels, *L* and *s* denote the large and the small subunits, respectively. Figures were generated with the

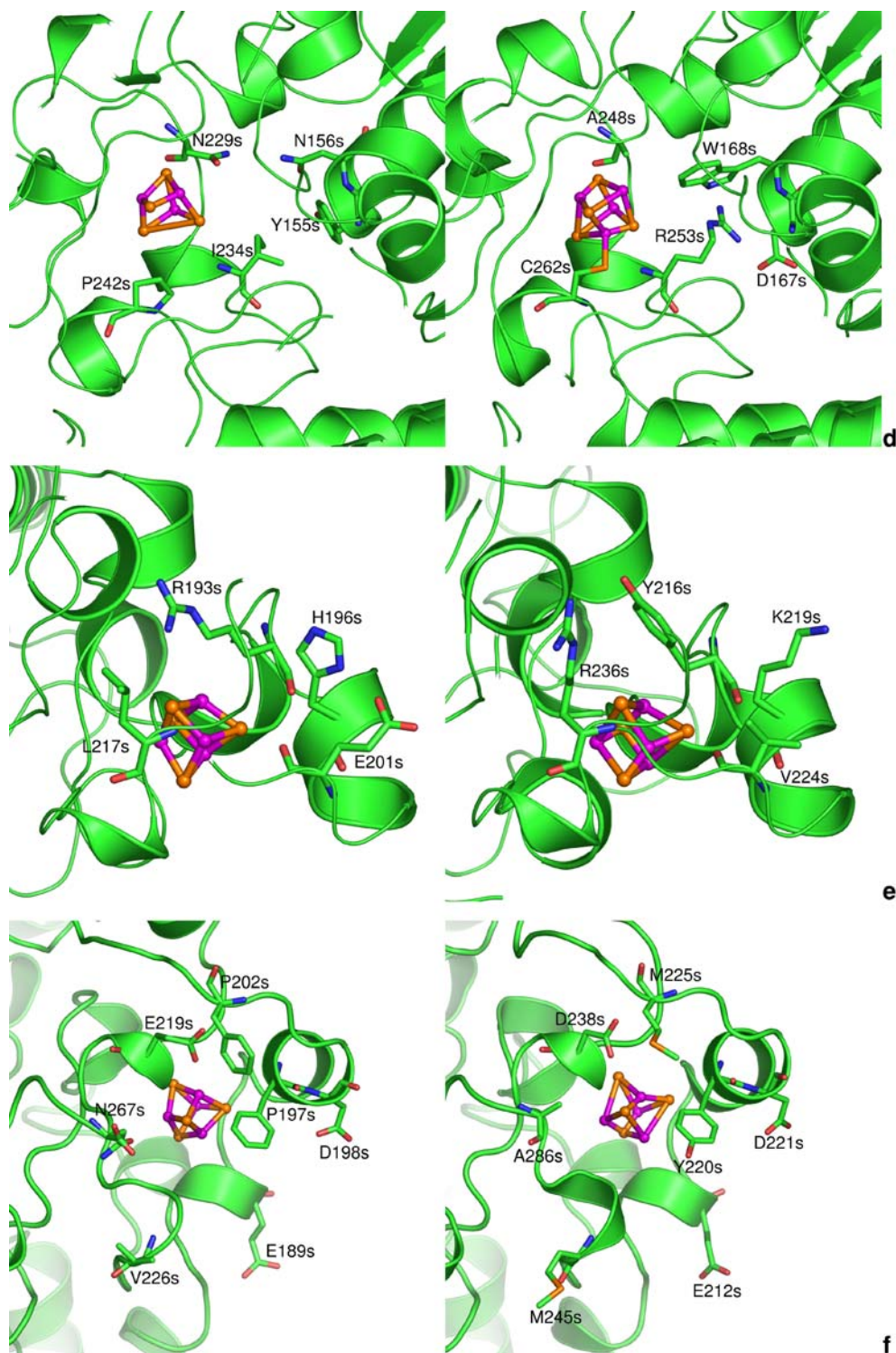
program Pymol [78]. **a** Three dimensional structure of the whole protein. The extra segment in the [NiFeSe] Hase is identified in the figure. **b** View of the active site. **c** View of the proximal [4Fe4S]^{2+/+} centre. **d** View of the medial [4Fe4S]^{2+/+} centre. **e** View of the distal [4Fe4S]^{2+/+} centre. **f** View of the Hase zone that interacts with the Tpl *c*₃

[NiFe] and [NiFeSe] Hase active-site models revealed similar structural and electronic properties, suggesting that the activity differences observed for the two kinds of Hases cannot be attributed to the S–Se substitution alone, and that the protein environment on the active site also plays an important role in tuning the catalytic properties of the enzymes [76]. The conserved differences

identified can thus have important consequences in terms of the reaction mechanism and redox potential of the metal centres.

In the large subunit, near the active site (Fig. 7b), [NiFeSe] Hases miss a salt bridge in comparison with [NiFe] Hases, due to the substitution of an aspartate (D123L in *DvM* [NiFe] Hase) by a serine (S117L in *DvH*

Fig. 7 (Contd.)



[NiFeSe] Hase). Thus, a three-centred salt bridge (R479L, D123L and D544L in *DvM* [NiFe] Hase) becomes two-centred (R422L and D487L in *DvH* [NiFeSe] Hase). Another difference in this zone is a slight displacement of the main chain, due to the replacement of a threonine (T85L in *DvM* [NiFe] Hase) by a proline (P79L in *DvH* [NiFeSe] Hase). This may be the reason why one of the cysteine ligands of the iron (C78L in *DvH* [NiFeSe] Hase) is slightly displaced in the [NiFeSe] Hase. This small deviation may have consequences in the catalytic mechanism.

In the small subunit, near the proximal $[4Fe4S]^{2+/1+}$ centre (Fig. 7c), a glutamate (E16s in *DvM* [NiFe] Hase) and a histidine (H13s in *DvM* [NiFe] Hase) are substituted by a glycine (G20s in *DvH* [NiFeSe] Hase) and a glutamine (Q17s in *DvH* [NiFeSe] Hase), respectively. The substitution of a charged residue (the glutamate) near the proximal centre, in the absence of other conjugated mutations, may have important consequences on its redox potential, increasing it. However, given that there is a simultaneous disappearance of a histidine, which by virtue of its proximity with the negatively charged glutamate is likely to be positively charged, it is difficult to predict the consequences of this substitution. Another interesting mutation, due to its proximity with the proximal centre, is the substitution of a glutamine (Q121s in *DvM* [NiFe] Hase) by a proline (P131s in *DvH* [NiFeSe] Hase), which induces a slight deviation of the main chain and increases the compactness of the structure near this centre.

Several differences are found near the medial $[4Fe4S]^{2+/1+}$ centre (Fig. 7d). Some of these occur at the surface of the protein with the net result of leading to a higher protection of this centre from the solvent in [NiFeSe] Hases. An isoleucine and a tyrosine (I234s and Y155s in *DvM* [NiFe] Hase) are substituted by an arginine and an aspartate (R253s and D167s in *DvH* [NiFeSe] Hase) forming salt bridges with other residues. Another interesting mutation is the substitution of an asparagine in [NiFe] Hases (N156s in *DvM* [NiFe] Hase) by a tryptophan residue (W168s in *DvH* [NiFeSe] Hase). To allow the insertion of the tryptophan in this place, another substitution occurs nearby, changing a larger asparagine (N229s in *DvM* [NiFe] Hase) by a smaller alanine (A248s in *DvH* [NiFeSe] Hase). In addition, a proline residue (P242s in *DvM* [NiFe] Hase) in the [NiFe] Hases is substituted by a cysteine (C262s in *DvH*

[NiFeSe] Hase) which binds the extra iron of the medial $[4Fe4S]^{2+/1+}$ centre.

Near the distal $[4Fe4S]^{2+/1+}$ centre several noteworthy point mutations were also identified (Fig. 7e). An arginine (R193s in *DvM* [NiFe] Hase) in the [NiFe] Hases is substituted by a tyrosine (Y216s in *DvH* [NiFeSe] Hase) in the [NiFeSe] Hases, but simultaneously, there is the replacement of a leucine (L217s in *DvM* [NiFe] Hase) by an arginine (R236s in *DvH* [NiFeSe] Hase). Therefore, a positive charge is maintained, not in sequence, but in spatial location. Additionally, a histidine (H196s in *DvM* [NiFe] Hase) in the [NiFe] Hases is substituted by a lysine (K219s in *DvH* [NiFeSe] Hase). This is an interesting case, because there may be an introduction of an extra positive charge, depending on the protonation state of the histidine. However, from the observation of the position of this histidine and taking into account its proximity to a negatively charged residue (E201s in *DvM*), it seems probable that the histidine is positively charged, in which case this mutation may not introduce significant electrostatic alterations.

The experimental results presented before suggest that the physiological partner for *DvH* [NiFeSe] and [NiFe]₁ Hases is the same cytochrome, the Tpl c₃. This suggests that the interaction zone between the [NiFeSe] Hase and this cytochrome is similar to the interaction zone found for [NiFe] Hases [77]. Indeed, analysis of the group of residues that were predicted to interact with the Tpl c₃ in this previous work shows that the acidic residues located at the surface as well as the hydrophobic ones located in the middle of the interaction zone are mostly conserved (or of the same kind) in both types of Hases (see Table 4, Fig. 7f).

Conclusions

A [NiFeSe] Hase was isolated as the major Hase in the membranes of the lactate/sulphate grown *DvH*. The enzyme is formed by two subunits with apparent molecular masses of 63 and 35 kDa by SDS gel, and contains selenium in equimolar amounts to Ni. It is isolated in an active, EPR-silent state and displays a very high H₂ production activity from reduced MV, which requires the presence of phospholipids. This Hase is present in the cell in two states: the majority is

Table 4 Residues in the interaction zone with the Tpl c₃ identified in the *D. gigas* Hase small subunit [77], and their corresponding residues in the other Hases small subunits analysed here

[NiFe] <i>D. gigas</i>	[NiFe] <i>DvMiyazaki</i>	[NiFeSe] <i>Dm. baculatum</i>	[NiFeSe] <i>DvH</i>
E216	E219	E234	D238
A264	N267	A282	A286
E195	D198	D218	D221
D186	E189	E209	E212
F199	F202	F222	M225
P194	F197	Y217	Y220
D223	V226	S241	M245

membrane-associated (the $[\text{NiFeSe}]_m$ form) and a minor amount is soluble (the $[\text{NiFeSe}]_s$ form). The large subunit of the $[\text{NiFeSe}]_m$ form displays a higher mass than predicted from the sequence, suggesting it is post-translationally modified, probably by the binding of a lipidic group at the N-terminus. The presence of such a group explains the membrane association of this Hase, the requirement of phospholipids for maximal activity, and the blockage of the large subunit to N-terminal sequencing. The soluble $[\text{NiFeSe}]_s$ form has a free N-terminal for the large subunit that starts with Gly12, and a considerably lower activity than the $[\text{NiFeSe}]_m$, which is relatively insensitive to the presence of phospholipids or detergent. The $[\text{NiFeSe}]_s$ Hase may be formed from the $[\text{NiFeSe}]_m$ Hase by cleavage of the lipidic group by a lipase encoded in the same locus as the $[\text{NiFeSe}]$ and $[\text{NiFe}]_1$ Hase genes, or by auto-proteolytic degradation as observed in aged preparations of the $[\text{NiFeSe}]_m$ form. The presence of $[\text{NiFeSe}]$ Hase in several forms (soluble and membrane-bound) has also been reported for *Dm. norvegicum* and *Dm. baculatum* [14]. Further studies underway are aimed at elucidating the nature of the post-translational modification of the *DvH* membrane-bound $[\text{NiFeSe}]$ and $[\text{NiFe}]_1$ Hases.

Sequence analysis shows that the *Desulfovibrionaceae* $[\text{NiFeSe}]$ Hases are distantly related to the $[\text{NiFe}]$ Hases present in the same organisms, and are more closely related to the $[\text{NiFe}]$ Hases from organisms like *C. hydrogenoformans*, *D. ethenogenes* or the sulphate-reducing bacterium *D. psychrophila*, which do not contain SeCys but have three $[\text{4Fe4S}]^{2+/1+}$ centres in the small subunit. It is common for SeCys-containing proteins that their Cys homologues can also be found in the same or different species, generally displaying a lower activity. Selenium compounds undergo much the same chemistry as their sulphur homologues and they are mostly metabolised by common pathways. However, selenium compounds are generally more reactive, particularly in redox reactions, and at physiological pH values the selenol group of SeCys is almost fully ionised ($\text{pK}_a < 5.2$) whereas the thiol group of Cys is largely protonated ($\text{pK}_a > 8$).

Studies with active-site models of $[\text{NiFe}]$ and $[\text{NiFeSe}]$ Hases suggest that the difference in activity between these two Hases cannot be attributed to the S–Se substitution alone [76]. A model for the structure of the *DvH* $[\text{NiFeSe}]$ Hase was generated and compared with available structures for other *Desulfovibrio* $[\text{NiFe}]$ Hases and the *Dm. baculatum* $[\text{NiFeSe}]$ Hase. This analysis permitted the identification of several conserved differences among $[\text{NiFe}]$ and $[\text{NiFeSe}]$ Hases, some of which are in residues close to the metal centres that may thus have a direct influence in the catalytic activity. Future site-directed mutagenesis studies are planned to address this question.

The presence of a signal peptide in the small subunit indicates that the $[\text{NiFeSe}]$ Hase is translocated to the periplasmic side of the membrane. However, in contrast

to most other periplasmic-uptake Hases, the $[\text{NiFeSe}]$ Hase does not have a membrane-bound cytochrome *b* as the electron acceptor, suggesting that its electron acceptor is a cytochrome *c*. Kinetic studies with the most abundant cytochromes *c* of *DvH* indicate that the physiological electron acceptor for the $[\text{NiFeSe}]$ Hase is the TpI c_3 , as observed for the $[\text{NiFe}]_1$ and $[\text{FeFe}]$ Hases of the same organism. However, the TpII c_3 , which is associated with a transmembrane redox complex, is also reduced with a significant rate. Thus, the difference between the three periplasmic-facing Hases of *DvH* is not in their electron acceptor. It is interesting to note that in the iron-reducing organisms like *Geobacter* or *Shewanella*, which contain an even higher cellular concentration of cytochromes *c* than *Desulfovibrio* (including cytochrome c_7 of the cytochrome c_3 family), the periplasmic Hases present do not use these cytochromes as electron acceptors but have instead a haem *b* subunit. Thus, the high abundance of Hases and TpI c_3 in the periplasm of *Desulfovibrio* seems to be related to the specific role of H_2 in the sulphate-reduction metabolism, and SRB possess several membrane-bound complexes for electron transfer from the periplasm to the cytoplasm that are unique to these organisms [13]. Several of these complexes include a periplasmic cytochrome *c* subunit that can accept electrons from the oxidation of H_2 in the periplasm via the TpI c_3 . The membrane association of the $[\text{NiFeSe}]$ and $[\text{NiFe}]_1$ Hases in *DvH* may facilitate the process of electron transfer from H_2 oxidation to the membrane menaquinone pool, involving one of these Hases, the TpI c_3 , HmcA or the TpII c_3 and their respective transmembrane complexes. Up to a third of the total amount of TpI c_3 in *DvH* is also found associated with the membrane fraction, even after washing of the membranes with low ionic strength buffer [20]. It is possible that a super-complex is formed between all proteins involved in this pathway, which may lead to optimised electron transfer and/or enhanced protein stability.

In conclusion, the *DvH* $[\text{NiFeSe}]$ Hase displays similar reactivity to the $[\text{NiFe}]_1$ Hase with *DvH* cytochromes *c* as the physiological electron transfer partners, pointing to a similar physiological function in the H_2 oxidation. The resistance of the $[\text{NiFeSe}]$ Hase to inactivation by oxygen may be a relevant property in terms of the advantage of this organism in having the two kinds of Hases. Further studies on the expression conditions of each Hase in *DvH* should shed some light into this issue.

Acknowledgements We would like to thank Mr. João Carita and the staff of the IBET Fermentation Plant for growing the bacterial cells, Mrs. M. Regalla for N-terminal sequence determinations, and Ms. Elisabete Pires for mass spectrometry analyses. We would also like to thank Dr. John Heidelberg from The Institute of Genomic Research for allowing us access to the *DvH* list of annotated genes prior to publication. This work was supported by FCT grants POCTI/ESP/44782/02 to I.A.C.P., POCTI/BME/32789/99 to C.M.S. and A.S.F.O., and POCTI/QUI/47866/02 to A.V.X. F.M.A.V. is supported by a FCT PhD grant (SFRH/BD/9187/2002).

References

1. Woodward J, Orr M, Cordray K, Greenbaum E (2000) *Nature* 405: 1014–1015
2. Hallenbeck PC, Benemann JR (2002) *Int J Hydrogen Energ* 27: 1185–1193
3. Kalia VC, Lal S, Ghai R, Mandal M, Chauhan A (2003) *Trends Biotechnol* 21:152–156
4. Nandi R, Sengupta S (1998) *Crit Rev Microbiol* 24:61–84
5. Armstrong FA (2004) *Curr Opin Chem Biol* 8:133–140
6. Jones AK, Sillery E, Albracht SPJ, Armstrong FA (2002) *Chem Commun* 8:866–867
7. Mertens R, Liese A (2004) *Curr Opin Biotechnol* 15:343–348
8. Schwartz E, Friedrich B (2003) In: Dworkin M et al. (ed) *The prokaryotes: an evolving electronic resource for the microbiological community*. Springer, Berlin Heidelberg New York. <http://link.springer-ny.com/link/service/books/10125/>. New York,
9. Odom JM, Peck HD Jr (1981) *FEMS Microbiol Lett* 12:47–50
10. Vignais PM, Billoud B, Meyer J (2001) *FEMS Microbiol Rev* 25: 455–501
11. Vignais PM, Colbeau A (2004) *Curr Issues Mol Biol* 6:159–188
12. Wu LF, Mandrand MA (1993) *FEMS Microbiol Rev* 10:243–269
13. Matias PM, Pereira IAC, Soares CM, Carrondo MA (2005) *Prog Biophys Mol Biol* 89:292–329
14. Fauque G, Peck HD Jr, Moura JJ, Huynh BH, Berlier Y, DerVartanian DV, Teixeira M, Przybyla AE, Lespinat PA, Moura I, LeGall J (1988) *FEMS Microbiol Rev* 4:299–344
15. Frey M, Fontecilla-Camps JC, Volbeda A (2001) In: Messerschmidt A, Huber R, Wieghardt K, Poulos T (eds) *Handbook of metalloproteins*, Wiley, New York, pp 880–896
16. Lemon BJ, Peters JW (2001) In: Messerschmidt A, Huber R, Wieghardt K, Poulos T (eds) *Handbook of metalloproteins*, Wiley, New York, pp 738–751
17. Voordouw G, Niviere V, Ferris FG, Fedorak PM, Westlake DWS (1990) *Appl Environ Microbiol* 56:3748–3754
18. Rossi M, Pollock WBR, Reij MW, Keon RG, Fu R, Voordouw G (1993) *J Bacteriol* 175:4699–4711
19. Pereira IAC, Romão CV, Xavier AV, LeGall J, Teixeira M (1998) *J Biol Inorg Chem* 3:494–498
20. Valente FMA, Saraiva LM, LeGall J, Xavier AV, Teixeira M, Pereira IAC (2001) *ChemBioChem* 2:895–905
21. Heidelberg J F, Seshadri R, Haveman SA, Hemme CL, Paulsen IT, Kolonay JF, Eisen JA, Ward N, Methe B, Brinkac LM, Daugherty SC, Deboy RT, Dodson RJ, Durkin AS, Madupu R, Nelson WC, Sullivan SA, Fouts D, Haft DH, Selengut J, Peterson JD, Davidsen TM, Zafar N, Zhou LW, Radune D, Dimitrov G, Hance M, Tran K, Khouri H, Gill J, Utterback TR, Feldblyum TV, Wall JD, Voordouw G, Fraser CM (2004) *Nat Biotechnol* 22: 554–559
22. Rodrigues R, Valente FM, Pereira IA, Oliveira S, Rodrigues-Pousada C (2003) *Biochem Biophys Res Commun* 306:366–375
23. Hedderich R (2004) *J Bioenerg Biomembr* 36:65–75
24. Casalot L, Valette O, De Luca G, Dermoun Z, Rousset M, de Philip P (2002) *FEMS Microbiol Lett* 214:107–112
25. Casalot L, De Luca G, Dermoun Z, Rousset M, de Philip P (2002) *J Bacteriol* 184:853–856
26. Pohorelic BK, Voordouw JK, Lojou E, Dolla A, Harder J, Voordouw G (2002) *J Bacteriol* 184:679–686
27. Romao CV, Pereira IA, Xavier AV, LeGall J, Teixeira M (1997) *Biochem Biophys Res Commun* 240:75–79
28. Lissolo T, Choi ES, LeGall J, Peck HD Jr (1986) *Biochem Biophys Res Commun* 139:701–708
29. Yagi T (1970) *J Biochem (Tokyo)* 68:649–657
30. Rieder R, Cammack R, Hall DO (1984) *Eur J Biochem* 145:637–643
31. Teixeira M, Fauque G, Moura I, Lespinat PA, Berlier Y, Prickril B, Peck HD, Xavier AV, Legall J, Moura JGG (1987) *Eur J Biochem* 167:47–58
32. Voordouw G, Menon NK, LeGall J, Choi ES, Peck HD Jr, Przybyla A E (1989) *J Bacteriol* 171:2894–2899
33. He SH, Teixeira M, LeGall J, Patil DS, Moura I, Moura JJ, DerVartanian DV, Huynh BH, Peck HD Jr (1989) *J Biol Chem* 264: 2678–2682
34. Pereira AS, Franco R, Feio MJ, Pinto C, Lampreia J, Reis MA, Calvete J, Moura I, Beech I, Lino AR, Moura JJ (1996) *Biochem Biophys Res Commun* 221:414–421
35. Eidsness MK, Scott RA, Prickril BC, DerVartanian DV, Legall J, Moura I, Moura JJ, Peck HD Jr (1989) *Proc Natl Acad Sci USA* 86: 147–151
36. Garcin E, Vernede X, Hatchikian EC, Volbeda A, Frey M, Fontecilla-Camps JC (1999) *Structure* 7:557–566
37. Sorgenfrei O, Duin EC, Klein A, Albracht SP (1996) *J Biol Chem* 271: 23799–23806
38. Sorgenfrei O, Duin EC, Klein A, Albracht SP (1997) *Eur J Biochem* 247:681–687
39. Legall J, Payne WJ, Chen L, Liu MY, Xavier AV (1994) *Biochimie* 76: 655–665
40. Ackrell BAC, Asato RN, Mower HF (1966) *J Bacteriol* 92:828–838
41. Wardi AH, Michos GA (1972) *Anal Biochem* 49:607–609
42. Teixeira M, Campos AP, Aguiar AP, Costa HS, Santos H, Turner DL, Xavier AV (1993) *FEBS Lett* 317:233–236
43. Pandey A, Andersen JS, Mann M (2000) *Science's Stke* 37:1–12
44. Gonnet F, Lemaitre G, Waksman G, Tortajada J (2003) *Proteome Sci* 1:2
45. Peck HD Jr, Gest H (1956) *J Bacteriol* 71:70–80
46. Lallamaharajh WV, Hall DO, Cammack R, Rao KK, Legall J (1983) *Biochem J* 209:445–454
47. Bjorklof K, Zickermann V, Finel M (2000) *FEBS Lett* 467:105–110
48. Sanchez R, Sali A (1997) *Curr Opin Struct Biol* 7:206–214
49. Marti-Renom MA, Stuart AC, Fiser A, Sanchez R, Melo F, Sali A (2000) *Annu Rev Biophys Biomol Struct* 29:291–325
50. Sali A, Blundell TL (1993) *J Mol Biol* 234:779–815
51. Laskowski RA, Macarthur MW, Moss DS, Thornton JM (1993) *J Appl Crystallogr* 26:283–291
52. Meur J, Kuettner HC, Zhang JK, Hedderich R, Metcalf WW (2002) *Proc Natl Acad Sci USA* 99:5632–5637
53. Fox JD, Kerby RL, Roberts GP, Ludden PW (1996) *J Bacteriol* 178: 1515–1524
54. Haveman SA, Brunelle V, Voordouw JK, Voordouw G, Heidelberg JF, Rabus R (2003) *J Bacteriol* 185:4345–4353
55. Hayashi S, Wu HC (1990) *J Bioenerg Biomembr* 22:451–471
56. Makula RA, Finnerty WR (1974) *J Bacteriol* 120:1279–1283
57. Volbeda A, Martin L, Cavazza C, Matho M, Faber BW, Roseboom W, Albracht SP, Garcin E, Rousset M, Fontecilla-Camps JC (2005) *J Biol Inorg Chem* 10:239–249
58. Sebban C, Blanchard L, Bruschi M, Guerlesquin F (1995) *FEMS Microbiol Lett* 133:143–149
59. Costa C, Teixeira M, LeGall J, Moura JGG, Moura I (1997) *J Biol Inorg Chem* 2:198–208
60. Pieulle L, Haladjian J, Bonicel J, Hatchikian EC (1996) *Biochem Biophys Acta* 1273:51–61
61. Matias PM, Coelho R, Pereira IAC, Coelho AV, Thompson AW, Sieker LC, LeGall J, Carrondo MA (1999) *Structure* 7:119–130
62. Aubert C, Brugna M, Dolla A, Bruschi M, Giudici-Ortoni MT (2000) *Biochim Biophys Acta* 1476:85–92
63. Matias PM, Coelho AV, Valente FMA, Ptacido D, LeGall J, Xavier AV, Pereira IAC, Carrondo MA (2002) *J Biol Chem* 277:47907–47916
64. Frazão C, Sieker L, Sheldrick G, Lamzin V, LeGall J, Carrondo MA (1999) *J Biol Inorg Chem* 4:162–165
65. Czjzek M, Guerlesquin F, Bruschi M, Haser R (1996) *Structure* 4: 395–404
66. Peck HDJ, Lissolo T (1988) In: Cole JA, Ferguson SJ (eds) *The nitrogen and sulphur cycles*. Cambridge University Press, Cambridge, pp 99–132
67. Rohde M, Furstenuau U, Mayer F, Przybyla AE, Peck HD Jr, Le Gall J, Choi ES, Menon NK (1990) *Eur J Biochem* 191:389–396

68. Casalot L, Rousset M (2001) *Trends Microbiol* 9:228–237
69. Price MN, Huang KH, Alm EJ, Arkin AP (2005) *Nucleic Acids Res* 33: 880–892
70. Akoh CC, Lee GC, Liaw YC, Huang TH, Shaw JF (2004) *Prog Lipid Res* 43:534–552
71. Page CC, Moser CC, Chen X, Dutton PL (1999) *Nature (London)* 402: 47–52
72. Bingemann R, Klein A (2000) *Eur J Biochem* 267:6612–6618
73. Rousset M, Montet Y, Guigliarelli B, Forget N, Asso M, Bertrand P, Fontecilla-Camps JC, Hatchikian EC (1998) *Proc Natl Acad Sci USA* 95:11625–11630
74. Higuchi Y, Yagi T, Yasuoka N (1997) *Structure* 5:1671–1680
75. Volbeda A, Charon MH, Piras C, Hatchikian EC, Frey M, Fontecilla-Camps JC (1995) *Nature* 373:580–587
76. De Gioia L, Fantucci P, Guigliarelli B, Bertrand P (1999) *Int J Quantum Chem* 73:187–195
77. Matias PM, Soares CM, Saraiva LM, Coelho R, Morais J, Le Gall J, Carrondo MA (2001) *J Biol Inorg Chem* 6:63–81
78. Delano W (2003) Delano Scientific LLC, San Carlos